Astron. Astrophys. 285, 333–343 (1994)

ASTRONOMY AND ASTROPHYSICS

Solar radiation pressure perturbations for Earth satellites

II. An approximate method to model penumbra transitions and their long–term orbital effects on LAGEOS

D. Vokrouhlický [1,2], **P. Farinella** [3,4], **and F. Mignard** [2]

[1] Astronomical Institute, Charles University, Švédská 8, 15000 Prague 5, Czech Republic
[2] Observatoire de la Côte d'Azur, Dept. CERGA, URA CNRS 1360, Av. N. Copernic, F-06130 Grasse, France
[3] Gruppo di Meccanica Spaziale, Dipartimento di Matematica, Università di Pisa, Via Buonarroti 2, I-56127 Pisa, Italy
[4] Observatoire de la Côte d'Azur, Dept. Cassini, URA CNRS 1362, B.P. 229, F-06304 Nice Cedex 4, France

Received 25 August 1993 / Accepted 21 October 1993

Abstract. We have developed an approximate version of our theory (Vokrouhlický et al. 1993c) for the perturbing force due to solar radiation pressure undergone by artificial Earth satellites when they cross the penumbra zones. The relative discrepancies in the instantaneous acceleration values with respect to the complete theory are generally smaller than 1%, and no systematic pattern resulting into spurious long–term perturbations arises. At the same time, the approximate approach leads to a considerable gain in the computing time needed for evaluating the perturbing force, typically an improvement by a factor 10 to 50. As a consequence, the theory is now suitable for implementation in the orbit analysis/determination codes used in space geodesy. Moreover, it can be applied to study the long–term perturbations associated with the penumbra effect on the orbital semimajor axis of LAGEOS. We have thus assessed that the additional long–term along–track perturbations resulting from the penumbra transition, with respect to those predicted by a simple step–like model, are of the order of several times 10^{-13} m/s^2, smaller than — but not negligible when compared to — the other radiative forces which contribute to LAGEOS' semimajor axis residuals. The long–term perturbations are due to the asymmetry between entrance into and exit from the Earth's shadow, resulting from different conditions of the atmosphere at opposite sides of the Earth. It appears likely that this penumbra effect plays a role in determining the relative sizes of the along–track acceleration spikes which have been detected when LAGEOS crosses the Earth's shadow.

Key words: celestial mechanics – space vehicles – atmospheric effects

Send offprint requests to: D. Vokrouhlický (Prague address)

1. Introduction

Radiative perturbations, in the context of artificial satellite dynamics, can be divided into two basic categories:

(i) *external effects*, due to the fact that the satellite is "bathed" into the radiative field of various external sources, such as the Sun and the Earth — they include direct solar radiation pressure, the force due to sunlight reflected or scattered from the Earth's surface/atmosphere, and that caused by infrared radiation emitted by the Earth;

(ii)*internal effects*, arising when the satellite itself emits radiation to some extent anisotropically, hence it undergoes a recoil acceleration — this is the case for the thermal trust or Yarkovsky–type force and the Poynting–Robertson effect.

In the last few decades, all of these effects have drawn the attention of celestial mechanicians and space dynamicists, in relation with the analysis of short– as well as long–term perturbations in satellite trajectories (for a review, see Milani et al. 1987). The theory of non–gravitational perturbing forces has been particularly refined in the wake of the discovery of puzzling residual (i.e., unmodelled) accelerations in the orbit of the laser–tracked satellite LAGEOS (Smith & Dunn 1980; Rubincam 1982). The radiative forces listed above have played a special role in the ongoing discussion — and the partial solution achieved so far — of the problems related to identifying the physical mechanisms responsible for the observed LAGEOS residuals (Anselmo et al. 1983a; Rubincam 1987, 1988, 1990; Barlier et al. 1986; Rubincam & Weiss 1986; Afonso et al. 1989).

In this paper, we will focus on some aspects of the perturbing force due to direct solar radiation pressure. As explained in Paper I (Vokrouhlický et al. 1993c), the treatment of the external radiative effects can be conveniently split into two steps:

(i) a characterization of the radiative field in which the satellite is plunged, depending only on the properties of the radiation source;

(ii) a model for the interaction of the radiation flux with the satellite's surface, possibly including the self–shadowing and multiple–reflection effects undergone by spacecraft with a complex shape (Anselmo et al. 1983b; Klinkrad et al. 1990).

A general mathematical formalism suitable for this splitting of the problem has been described in Vokrouhlický et al. (1993a). Throughout this paper we will deal with the treatment of direct solar radiation pressure restricting ourselves to step (i) — i.e., we will assume that the satellite has the simplest possible shape and surface properties: a nearly–spherical shape and quasi–isotropical optical properties. This is actually a good approximation for LAGEOS. Anyway, we stress that the two steps quoted above are conceptually separated, so that all the results presented in the following can be extended to the more general case of complex–shaped and/or optically anisotropical satellites.

Modelling the perturbative effect of direct solar radiation pressure on the orbit of a spherical satellite is rather straightforward, but for the passages from full sunlight to the Earth's shadow and *vice versa*. These will be referred to below as the *penumbra transitions*. These transitions take place only when the satellite's orbit crosses the Earth's shadow, and even then they last at most a few percent of the orbital period. However, in special situations this tiny effect acting over short time intervals can play a significant role in the observed dynamical behaviour of satellites. Such is the case for the accelerometric experiments devoted to direct measurements of the non–gravitational forces acting on spacecraft (see e.g. Peřestý & Sehnal 1992). In this case, the time dependence of the solar radiation pressure during the penumbra transitions can be directly measured and compared with model predictions. A more subtle effect may be due to the fact that the along–track component of the radiative force behaves asymmetrically during the entry and exit transitions, hence it does not average out over one orbital revolution. In this case the perturbing effect on the orbital semimajor axis accumulates and long–term variations are generated. In Sect. 3, we will give an example of this by analysing the case of LAGEOS' acceleration residuals.

Let us recall some general properties of the penumbra effect. Already in the 60's it was recognized by Link (1962, 1969) that the essential role in determining the time dependence of the radiative force during the penumbra transitions is played by atmospheric processes, whereas the gradual eclipsing of the finite–size solar disk by the solid Earth is of minor importance. The optical properties of the atmosphere affect the solar radiation flux in two different ways: (i) the differential geometric refraction of separate solar rays causes them to diverge, implying that the net solar flux is decreased throughout the penumbra phase, which on the other hand has a longer duration (again due to refraction); (ii) the interaction of the solar radiation with the atmosphere decreases the radiative flux owing to absorption and scattering processes.

With the exception of a full treatment of atmospheric scattering, which would be extremely complex, we have shown in Paper I that all the atmospheric effects can be described by a realistic but still tractable theory. However, in Paper I we warned the readers that the large computing time requirements of the calculations needed by this formulation of the theory might be a serious obstacle to its wide application to concrete orbit analysis problems. This was a significant drawback of the method, since a realistic treatment of the penumbra effect would be quite useful in the codes which are commonly used for reduction of tracking data and orbit determination, for instance in the frame of space geodesy experiments (e.g. Fliegel et al. 1992). This conclusion is strengthened by the fact that in Paper I we confirmed Link's finding that the introduction of atmospheric refraction, absorption and scattering in the penumbra effect modifies in a very significant way the conclusions derived from the simpler approach, assuming the gradual disappearance of the undistorted solar disk behind the horizon.

Therefore, in this paper we present a simplified version of our theory of the penumbra effect, which does not degrade significantly the accuracy of the more complete formulation of it, while it leads to considerable improvements from the point of view of the computing efficiency. This simplified version is not based on a rigorous mathematical search for approximations, but is somewhat empirical and validated by numerical testing. The results of a number of careful tests have shown that the perturbing accelerations predicted by the approximate approach are within 1% of those computed by the complete theory (see Sect. 3). At the same time, we have achieved computing time savings by a factor typically ranging between 10 and 50. Thus, we hope that this computer effective version of the theory has become suitable for implementation in the procedures routinely used for satellite orbit analysis and determination.

The remainder of this paper is organized as follows: in Sect. 2 we introduce the approximate version of the penumbra theory, and explain why it speeds up considerably the computations. In Sect. 3 we discuss the accuracy of the theory and apply it to analyse possible long–term effects on the semimajor axis of LAGEOS. Some conclusions and open problems are summarized in Sect. 4.

2. Approximate penumbra effect theory

2.1. General formulation of the theory

The mathematical technique used throughout this series of papers has been spelled out in detail in Sect. 2 of Paper I. Since the use of this technique was not previously widespread in the framework of satellite dynamics and geodesy, we suggest the reader to give a look at Paper I in order to follow the arguments of the present work. Here, we will just give a short outline of those aspects of the theory which are not specifically connected with the penumbra effect, but are necessary to introduce further developments.

(1) Characterization of the radiation source. A realistic model of the penumbra transitions requires that the Sun is considered as an extended source of radiation. A spherical solar model is enough for our purposes, but we have to include some treatment of the limb darkening effect. Throughout this paper we will make use of integrated radiative quantities (intensity, flux), neglecting the frequency dependence of the integrands. This is consistent with accounting for limb darkening through the second Eddington approximation for a solar grey atmosphere (Mihalas 1970), that yields

$$I_\odot(\mu) = F_\odot \; \Psi_\odot(\mu) \; , \tag{1}$$

with

$$\Psi_\odot(\mu) = \frac{3}{4}\Big[\frac{7}{12} + \frac{1}{2}\mu + \mu\big(\frac{1}{3} + \frac{1}{2}\mu\big)\ln\big(\frac{1+\mu}{\mu}\big)\Big] \; .$$

Here $I_\odot$ is the radiative intensity, μ is the cosine of the angle between the direction of emission and the normal to the solar surface, and $F_\odot$ represents the astrophysical radiative flux emerging through the solar atmosphere. The quantity $F_\odot$ is related to the solar constant $\Phi_\odot$ through the relationships:

$$F_\odot = \frac{\Phi_\odot}{2\pi \mathscr{F}(\bar\rho_1)} \; ,$$

$$\mathscr{F}(\bar\rho_1) = \bar\rho_1^2 \int_{\bar\rho_1}^{1} d\mu'(\mu' - \bar\rho_1)(1 - \mu'\bar\rho_1) \\ \zeta^{-2}(\mu', \bar\rho_1)\Psi_\odot[(\mu' - \bar\rho_1)\zeta^{-1/2}(\mu', \bar\rho_1)] \; ,$$

$$\zeta(\mu', \bar\rho_1) = 1 - 2\bar\rho_1\mu' + \bar\rho_1^2 \; ,$$

where $\bar\rho_1$ denotes the radius of the solar photosphere in Astronomical Units (see Paper I, Secs. 2 and 3).

(2) Reference frames. The orbital elements of the satellite are referred to the commonly used inertial frame (X, Y, Z) whose X–axis is oriented toward the vernal equinox at some epoch, whereas the XY–plane coincides with the equatorial plane at the same epoch and the Z–axis is close to the Earth's rotation vector.

To evaluate the radiative force, on the other hand, it is convenient to use the so–called *Sun–oriented* reference frame (x, y, z), whose axes are directed as follows: the z–axis is parallel to the satellite's geocentric radius vector, the xz–plane is the plane defined by the geocentric positions of the Sun and the satellite, and the x–axis is chosen such that $(\mathbf{s}\cdot\mathbf{x}) < 0$, where $\mathbf{s}$ is the unit vector in the direction of the Sun. We also use the angular spherical coordinates (θ, ϕ) defined in the Sun–oriented frame (θ being measured from the z–axis). This frame has the advantage that the y–component of the force due to solar radiation pressure always vanishes for symmetry reasons.

(3) Evaluation of the radiative force. Assuming a spherical shape of the satellite (see Sect. 1) and quasi–isotropical optical properties of its surface (Vokrouhlický et al. 1993a), the general expression for the satellite's acceleration due to interaction with the radiative field is

$$\boldsymbol{a} = \frac{A}{mc}\mathscr{C}_{\mathrm{R}}\boldsymbol{F} \; , \tag{2}$$

where A is the satellite's geometrical cross-section, c the velocity of light, m the satellite mass, $\mathscr{C}_{\mathrm{R}}$ a dimensionless coefficient depending on the surface optical properties and $\boldsymbol{F}$ the radiative vector flux defined in Paper I (see also Mihalas 1970) as

$$\mathbf{F} = \int_{(\theta,\phi)} d(\cos\theta)d\phi \; \boldsymbol{n}(\theta,\phi)\, I[\mu(\theta,\phi);\tau] \; . \tag{3}$$

Here $\boldsymbol{n}(\theta, \phi)$ is the unit vector specifying a given direction (i.e., $\boldsymbol{n}^T(\theta, \phi) = (\sin\theta\cos\phi, \sin\theta\sin\phi, \cos\theta)$ and I is the radiative intensity. The domain of integration of the right–hand side integral in Eq. (3) is determined by the local radiative field, namely it simply covers the whole range of (θ, ϕ) values for which $I \neq 0$ (by definition $I = 0$ out of the radiative field generated by the Sun). The two arguments in $I[\mu(\theta, \phi); \tau]$ denote two different physical effects: $\mu(\theta, \phi)$ is the same quantity appearing in Eq. (1), and its dependence on the chosen local direction (θ, ϕ) is related to the refraction (i.e., bending) of the sunlight rays in the Earth's atmosphere; τ denotes half the optical thickness of the atmosphere along a given ray (θ, ϕ), characterizing atmospheric processes such as absorption and simple scattering.

(4) Radiative force out of penumbra transitions. In this case there is no intervention of the atmospheric effects, and after simple algebra Eq. (3) leads to the following expressions for the two nonzero components of the radiative flux in the Sun–oriented frame:

$$F_{\mathrm{x}} = 2\pi F_\odot \mathscr{F}(\rho_1\zeta^{-1/2}(\cos\omega\rho_2))\sin\theta_{\mathrm{s}} \; , \\ F_{\mathrm{z}} = 2\pi F_\odot \mathscr{F}(\rho_1\zeta^{-1/2}(\cos\omega, \rho_2))\cos\theta_{\mathrm{s}} \; , \tag{4}$$

where

$$\theta_{\mathrm{s}} = \arcsin\big\{\sin\omega\zeta^{-1/2}(\cos\omega, \rho_2)\big\} \; ,$$

$$\rho_1 = \frac{R_\odot}{R} \; , \quad \rho_2 = \frac{r}{R} \; , \tag{5}$$

ω is the geocentric angular distance between the Sun and the satellite, r is the instantaneous geocentric distance of the satellite, R is the corresponding Earth–Sun distance, and $R_\odot$ is the solar radius.

(5) Atmospheric model. A model for the structure and the optical properties of the Earth's atmosphere is an essential component of the penumbra theory. As we did in Paper I, we shall basically adopt Garfinkel's (1944, 1967) model to compute the refractive effects and some simple formulae based on a formal solution of the radiative transfer equation (Mihalas 1970) for the scattering and absorption processes. The main difference with respect to Garfinkel's formulation is that we neglect the existence of an upper isothermal layer of the atmosphere, and take into account only its lower polytropic layer. This choice simplifies Garfinkel's formulae, as boundary conditions between the two layers are not needed, and does not degrade in a significant way the accuracy of the results (the upper layer gives rise to a refractive effect of the order of 5 arcseconds for a grazing ray; see Garfinkel 1944).

Instead of repeating the fairly complicated formulae given by Garfinkel, we just recall the basic properties of Garfinkel's model: (i) a spherically symmetric distribution for the atmospheric density; (ii) the Gladstone–Dale law for the air refractive index (i.e., an essentially linear relationship between refractive index and air density; see Garfinkel 1967); (iii) a perfect gas atmosphere with polytropic equation of state characterized by an index n. Under these assumptions, Garfinkel showed that the dependence of the refractive index κ on the altitude h can be expressed as

$$\kappa(h) = 1 + \alpha\left(1 - 2\gamma^2 \frac{h}{R_\oplus + h}\right)^n , \tag{6}$$

$$2\gamma^2 = \frac{g_0 R_\oplus}{(n+1)\mathscr{R} T_0} ,$$

where α is a model constant (giving the refraction index at the Earth's surface), g_0 is the acceleration of gravity at the surface, $\mathscr{R}$ is the gas constant for air, $R_\oplus$ is the Earth's radius, and T_0 is the surface temperature. The polytropic index n is derived from the bottom conditions of the atmosphere, namely its temperature gradient T_0'. The top boundary of the atmosphere is determined by the condition $\kappa(h_T) = 1$ (necessary for continuity of the refractive index); explicitly we have $h_T = R_\oplus(2\gamma^2 - 1)^{-1}$. For more comments on these polytropic models of the atmosphere, see also McCartney (1976).

In the following, some of the atmospheric parameters will be considered as constant: the Earth's radius, the gas constant, and the acceleration of gravity. Other parameters, which provide essentially the boundary conditions at the Earth's surface, will be assumed to be variable: (i) the surface temperature T_0; (ii) the surface pressure p_0; (iii) the surface temperature gradient T_0' (given in Kelvins per "gravitational meter"; see Garfinkel 1944, 1967); and (iv) the water vapor pressure in the air p', which gives raise to a "humidity correction" modifying the refractive index at the surface, i.e., the parameter α in Eq. (6). Although, rigorously speaking, the set of parameters (T_0, p_0, T_0', p') should be constant over the whole surface to ensure spherical symmetry and staticity of the atmosphere, we shall assume that each of them depends on the geographical latitude and longitude as well as on time, corresponding to temperature and pressure differences existing on the real Earth's surface. The error arising from this inconsistency can be safely assumed to be small.

The output of the atmospheric refraction model of interest here is limited to a single function, namely the refraction angle $R_\star(h)$ of the solar ray grazing the atmospheric layer at an altitude h.

2.2. Approximate theory for the penumbra transitions

In this section we introduce a new approximate approach to the treatment of the penumbra transitions, aiming primarily at: (i) retaining as much as possible of the accuracy of the complete theory developed in Paper I; (ii) devising a formulation capable of accelerating significantly the numerical computations.

It is worth noting that the most time–consuming element of the complete theory is the two–dimensional integration required for the numerical evaluation of the radiative flux — see Eq. (3). The essential idea of our approximation is to avoid this double integration and replace it by an integration on a single variable, taking advantage of a property of the integrand in Eq. (3): the fact that this function behaves in a similar way on different ϕ–slices, as defined in Paper I, i.e. on different ϕ = constant planes. Although this similarity does not apply exactly, it holds approximately. Quantitatively, the similarity property can be expressed for instance through the following statement: if $\theta_+(\phi)$ and $\theta_-(\phi)$ are respectively the minimum and maximum values of the θ coordinate for the solar disk edge in a given ϕ–slice, and $\theta_c(\phi)$ is the value corresponding to the ray emitted normally to the solar body in the same ϕ–slice (note that $\theta_c(\phi = 0)$ defines the direction of the subsolar point), then the function $(\theta_-(\phi) - \theta_c(\phi))/(\theta_c(\phi) - \theta_+(\phi))$ is not exactly constant for different values of ϕ, but is bounded within a limited interval. As noted in Sect. 2.1, the resulting radiative flux has no y–component, namely it lies in the $\phi = 0$ slice.

These observations lead us to formulate the following approximation: the radiative flux to be inserted in Eq. (2) can be expressed as

$$\boldsymbol{F}_{\rm app} = F_{\rm app} \boldsymbol{n}_{\rm app} . \tag{7}$$

Here $F_{\rm app}$ is the approximate magnitude of the flux, given by

$$F_{\rm app} = F_{\rm out} \frac{\Delta\theta}{(\Delta\theta)_{\rm out}} \langle \exp(-2\tau) \rangle , \tag{8}$$

where $F_{\rm out}$ is the magnitude of the radiative flux before the beginning (or after the end) of the penumbra transition, specified by a Sun–satellite geocentric angular separation $\omega_{\rm out}$, and $\Delta\theta$ is the apparent vertical size of the flattened solar disk during the penumbra transition. Eq. (8) amounts to say that the actual radiative flux is directly proportional to the vertical angular size of the flattened Sun. This is a reasonable assumption because, when the absorption is neglected, the illumination of the satellite is determined by the intensity of the light source and the solid angle of the light beam, that is by the apparent area of the source. As the refraction flattens the solar disk without changing its width, the solid angle subtended by the Sun is a linear function of $\Delta\theta$. The validity of this assumption is supported by extensive numerical checks, as summarized below.

From Eqs. (4)-(5) we obtain

$$F_{\rm out} = 2\pi F_\odot \mathscr{F}[\rho_1 \zeta^{-1/2}(\cos\omega_{\rm out}, \rho_2)] \approx \Phi_\odot , \tag{9}$$

$$\omega_{\rm out} = \frac{\pi}{2} - \Lambda_+(\Psi_T; r, R_\odot, R) , \tag{10}$$

where

$$\Lambda_\pm(\Psi; r, R_\odot, R) = \arcsin\left\{ \frac{\Psi}{r}\left(\rho_1 \pm \frac{\Psi}{R}\right) \mp \sqrt{\left[1 - \left(\frac{\Psi}{r}\right)^2\right]\left[1 - \left(\rho_1 \pm \frac{\Psi}{R}\right)^2\right]} \right\} , \tag{11}$$

$$\Psi(h) = (R_\oplus + h)\kappa(h) . \tag{12}$$

In Eq. (10) we used the notation $\Psi_T = \Psi(h_T) = R_\oplus + h_T$. Note that Eq. (9) provides a rigorous expression for the magnitude of the radiative flux, coinciding with the illumination of the satellite in full sunlight. This expression can be approximated with a sufficient accuracy by the solar constant.

The second factor in Eq. (8), $\Delta\theta/(\Delta\theta)_{\rm out}$, accounts for the decrease in the radiation flux due to the atmospheric refraction; it is just the ratio between the vertical width of the solar disk in the θ–coordinate at a given instant, and the same quantity out of the penumbra. Simple algebra leads to

$$(\Delta\theta)_{\rm out} = 2\rho_1\zeta^{-1}(\cos\omega_{\rm out}, \rho_2) \approx 2\rho_1 . \qquad (13)$$

To a sufficient accuracy this is the same as the apparent solar diameter, $\approx$ 30 arcminutes.

Now, when the refraction of the solar rays is significant the apparent shape of the Sun is no longer a plain disk and must be determined with care. We will not repeat the whole derivation of the solar disk's vertical width $\Delta\theta$, which is given in Paper I; we only overview the formulae needed to determine this quantity. For this purpose, the following system of equations

$$\frac{\Psi(h)}{r} = \frac{\sin\varpi(h)\sqrt{\zeta\left(\cos\varpi(h), \rho_2\right) - \rho_1^2} \pm \rho_1\left(\rho_2 - \cos\varpi(h)\right)}{\zeta\left(\cos\varpi(h), \rho_2\right)} \qquad (14)$$

$$\varpi(h) = \omega - 2R_\star(h) , \quad \Psi(h) = (r+h)\kappa(h) ,$$

has to be solved iteratively for $h_\pm$ (the two signs correspond to the uppermost and lowermost rays defining the solar disk). Then, by means of the relationship

$$\Psi(h) = r\sin\theta , \qquad (15)$$

one obtains the corresponding values of the θ angle. Combining Eqs. (14) and (15) we finally obtain

$$\cos\Delta\theta = \left\{\frac{\Psi(h_+)\Psi(h_-)}{r^2} + \sqrt{\left[1 - (\frac{\Psi(h_+)}{r})^2\right]\left[1 - (\frac{\Psi(h_-)}{r})^2\right]}\right\} \qquad (16)$$

for the vertical width of the solar disk.

The last factor in Eq. (8) originates from physical processes in the atmosphere, connected with the light–air interaction. It is defined as

$$\langle\exp(-2\tau)\rangle = \int_{\theta_+}^{\theta_-} d\theta \exp[-2\tau(\theta)] , \qquad (17)$$

i.e., it represents the averaged damping of the radiation flux coming from the vertical solar slice $\phi = 0$. To better explain this, we recall that the formal solution of the radiative transfer equation can be written as

$$I[\mu(\theta,\phi);\tau] = I^{(0)}[\mu(\theta,\phi)]\exp(-2\tau) , \qquad (18)$$

where $I^{(0)}(\mu(\theta,\phi))$ is the radiative intensity when the atmospheric attenuation (but not the ray bending in the atmosphere) is neglected, and τ is half of the optical thickness of the atmosphere, given by the integral

$$\tau = \int ds\, \chi(s) , \qquad (19)$$

which is extended over half the optical path of the rays in the atmosphere. If one assumes a constant absorption coefficient $\chi(h) = \chi^\star$ and neglects the bending of rays in the atmosphere, Eq. (19) gives

$$\tau^\star = \chi^\star\sqrt{(h_{\rm T} - h)(h_{\rm T} + h + 2R_\oplus)} . \qquad (20)$$

For Rayleigh scattering referred at the 550 nm wavelength, we have $\chi^\star = 1.162\times10^{-5}$ m^{-1} (McCartney 1976). Note that we are implicitly including in the theory only single–scattering processes, as a full treatment of the scattering problem would lead to much more complicated results (see Chandrasekhar 1960; van de Hulst 1980).

However, as shown in Paper I, assuming a constant absorption coefficient would corrupt the theory. Instead, we have adopted a suitable correction factor accounting for the variability of the absorption coefficient with altitude. Specifically, we assume a linear relationship between $\chi(h)$ and the atmospheric density $\rho(h)$, which is correct for the Rayleigh scattering (McCartney 1976). Taking into account the polytropic structure of the atmosphere and the definition (19), we obtain for the half–optical thickness

$$\tau = \tau^\star\int_0^1 d\xi\left[1 - 2\gamma^2\left(1 - \sigma(\tau^\star,\xi)^{-1/2}\right)^n\right] , \qquad (21)$$

with

$$\sigma(\tau^\star,\xi) = (\xi^2 - 1)\frac{\tau^{\star2}}{R_\oplus^2\chi^{\star2}} + (1 + \frac{h_{\rm T}}{R_\oplus})^2 .$$

The attenuation factor to be inserted in Eqs. (17)–(18) is then given by

$$\exp\left(-2\tau(\theta)\right) = \exp\left[-2\tau_\star\left(h\left(\theta\right)\right)\right] f_{\rm alt}\left[\tau_\star\left(h\left(\theta\right)\right)\right] , \qquad (22)$$

where the correction factor accounting for the altitude dependence of the absorption coefficient is

$$f_{\rm alt}(\tau^\star) = \exp\left\{2\tau^\star\left[1 - \int_0^1 d\xi\left[1 - 2\gamma^2\left(1 - \sigma(\tau^\star,\xi)^{-1/2}\right)\right]^n\right]\right\} . \qquad (23)$$

Summarizing the first part of our approximation formula (8), providing the magnitude of the radiative flux, we shall translate it into words, in order to clarify the physical meaning of the different terms:

$$\begin{pmatrix}\text{magnitude of}\\ \text{the radiative flux}\end{pmatrix} = \overbrace{\begin{pmatrix}\text{reference value of}\\ \text{the radiative flux}\end{pmatrix}}^{\text{characteristic flux value}} \times \overbrace{\begin{pmatrix}\text{compression factor}\\ \text{of the solar disk}\end{pmatrix}}^{\text{accounts for refractive effects}} \times \overbrace{\begin{pmatrix}\text{averaged absorption}\\ \text{over vertical solar slice}\end{pmatrix}}^{\text{accounts for physical effects}}$$

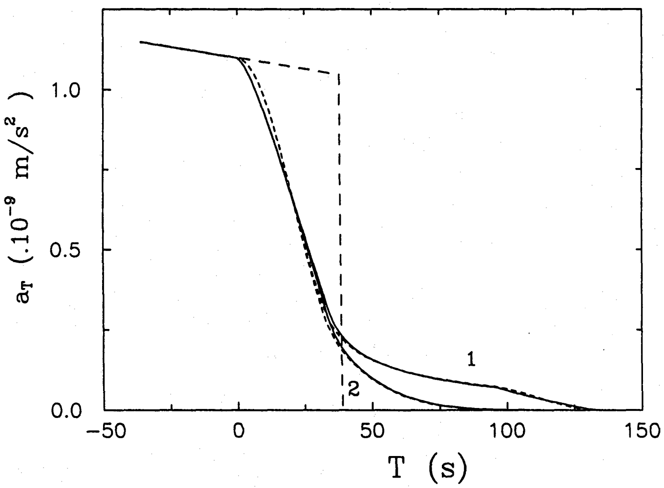

Fig. 1. The transverse acceleration component a_T (units 10^{-9} m/s^2) due to solar radiation pressure on the LAGEOS satellite, vs. time measured (in seconds) since the beginning of a penumbra entry transition. The figure compares the results based on the complete theory (dashed curve) to those based on the approximate approach described in the text (solid curve). The label 1 refers to calculations taking into account only the effects of atmospheric refraction, while curves labelled 2 include atmospheric Rayleigh scattering with altitude dependence of the extinction coefficient χ. Results from the rough approximation assuming a step–like transition are also shown. The following standard values for the parameters describing the atmospheric conditions were used: T_0 = 273.15 K, p_0 = 760 mm Hg, T_0' = −0.005694 K/m', p' = 0 mm Hg (see Garfinkel 1967)

Let us now turn to the problem of the orientation of the radiative flux vector, specified in Eq. (7) by the unit vector $\boldsymbol{n}_{\rm app}$. The only rigorous information we have on this issue is the solar disk symmetry under the transformation $\phi \rightarrow -\phi$, resulting in a zero y–component of the flux. Out of the penumbra phases, the direction of the radiative flux coincides with the direction of the solar ray emitted by the disk's center. We assume that the same property holds during the penumbra transitions as well, and then use the subsolar direction for the orientation of the radiative flux vector. Although this is not supported by any theory, numerical evidence to be presented in the following indicates that this choice is a good compromise. Anyway, it is clear that the true direction cannot differ from the assumed one by more that one tenth of the apparent solar diameter, that is some 3 arcminutes, producing a maximum error of the order of 10^{-3} in the projections of the force required to derive its components with respect to the orbit.

Thus, the unit direction vector $\boldsymbol{n}_{\rm app}$ in Eq. (7) takes the following form: $\boldsymbol{n}^{\rm T}_{\rm app} = (\sin\theta_{\rm m}, 0, \cos\theta_{\rm m})$, where $\theta_{\rm m}$ corresponds to the solar ray emitted normally to the solar body. Using the formulae given in Paper I, we obtain the set of equations

$$\frac{\Psi(h)}{r} = \sin\tilde{\omega}(h)\zeta^{-1}\left[\cos\tilde{\omega}(h), \rho_2\right] \ , \qquad (24)$$
$$\varpi(h) = \omega - 2R_\star(h) \ , \quad \Psi(h) = (r+h)\kappa(h) \ .$$

As we already did with Eq. (14), the numerical solution h of Eq. (24) can be combined with the simple relationship

$$\sin\theta_{\rm m} = \frac{\Psi_{\rm m}(h)}{r} \ ,$$

to provide the value of $\theta_{\rm m}$.

This completes the description of the approximate approach introduced in this paper. Mathematically, it just consists in substituting the complex integral (3) with Eq. (7).

Fig. 1 compares in a specific case (transverse acceleration component on the LAGEOS satellite during a penumbra entry transition) the results of the complete and approximate versions of our theory. We have used two very different atmospheric models: case 1 includes only refraction effects with no absorption and scattering, case 2 includes Rayleigh scattering together with the altitude decrease of the absorption coefficient, as discussed above. In both cases, the two versions of the theory yield remarkably close results, especially when compared with the rough step–like transition model commonly used in orbit analysis work.

We stress, however, that our approximate scheme, although based on plausible and intuitive arguments, cannot be rigorously justified. We have not specified any "small parameter" in the theory which may control the deviations of the approximate approach from the complete solution. In this situation, it is important to test our approximation in a quantitative way, providing a reliable statistical characterization of the discrepancies between the results of the two versions of the theory. For this purpose, we have defined the dimensionless quantity

$$\delta = \frac{\sqrt{\langle(\delta\boldsymbol{a})^2\rangle}}{\langle a\rangle} \ , \qquad (25)$$

where

$$\langle(\delta\boldsymbol{a})^2\rangle = \int_{\mathscr{P}}[\delta\boldsymbol{a}(M)]^2 dM \quad , \quad \langle a\rangle = \int_{\mathscr{P}} a(M)dM \ , \qquad (26)$$

$\mathscr{P}$ represents the interval in mean anomaly M affected by the penumbra effects, a is the magnitude of the perturbing acceleration due to the radiative force and $\delta\boldsymbol{a}$ is the vector difference between the more accurate value of the acceleration computed using the complete penumbra theory and the approximate value given by Eq. (7). The integration limits defined by the penumbra interval $\mathscr{P}$ can be computed analytically from the corresponding range in the ω geocentric angular distance between the Sun and the satellite, as explained in Paper I (Sect. 4.1), and the numerical calculation of integrals (26) is carried out by using a small enough step in M to avoid significant errors.

Figure 2 shows the distribution of the quantity δ for different atmospheric conditions, again for the orbit of LAGEOS. For both atmospheric models already used to derive Fig. 1, we have performed 200 runs with random choices of the atmospheric parameters (T_0, p_0, T_0', p'). No value of δ exceeded 1%, confirming the reliability of the approximate theory. The distribution of δ is Gaussian–like, with average values of about 0.5% and 0.65% for the two atmospheric models. These average values represent in a way the "systematic error" introduced by the approximate theory; this is somewhat larger when the atmospheric absorption is included, but the difference is of marginal significance.

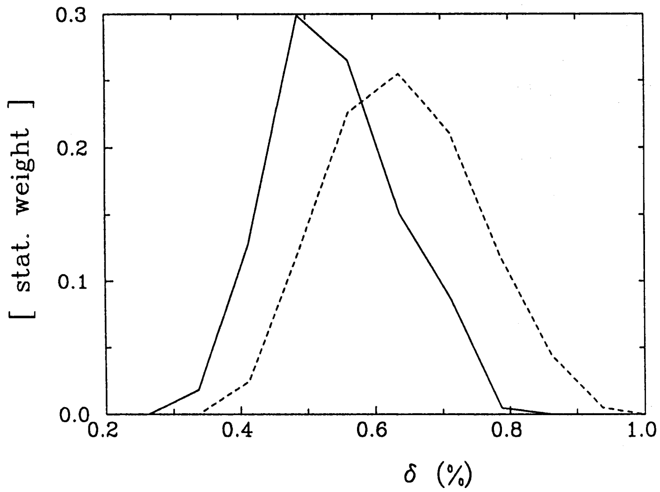

Fig. 2. Distribution of the δ quantity defined in the text to specify the relative discrepancy between the complete and the approximate versions of the theory. The solid curve refers to the no–absorption atmospheric model, the dashed one to the case when altitude–dependent Rayleigh extinction is included. The distributions have been derived from 200 runs each, carried out with random values of the atmospheric parameters, chosen in the following intervals: $T_0 \in (-20, 20)$°C, $p_0 \in (730, 790)$ mm Hg, $T_0' \in (-6.494, -4.894) \times 10^{-3}$ °K/m', $p' \in (0, 30)$ mm Hg

We have carried out similar computations for other satellites, ranging from low–altitude to geostationary orbits. In all cases the results are nearly the same as those shown in Fig. 2, showing in a convincing way that our approximation is uniformly accurate, independently of both the atmospheric conditions and the chosen orbit.

3. Penumbra effect and long–term LAGEOS' semimajor axis residuals

We shall now take advantage of the approximate approach presented in Sect. 2 to address a particular problem: the possible role of the penumbra effect in contributing to LAGEOS' orbital residuals. As we will show later, without our simplification of the theory, this problem would hardly be tractable.

The puzzle of LAGEOS' semimajor axis residuals arose soon after the earliest analyses of the laser tracking data specifically aimed at long–arc orbit determination (e.g. Smith & Dunn 1980). Today the problem can be considered as solved only in part. The observed secular semimajor axis decay appears to be due to a mixture of thermal thrust and neutral/charged–particle drag (Rubincam 1990), although the relative importance of the two mechanisms is somewhat uncertain. However, the debate is still open on the related issue of the long–periodic semimajor axis residuals and the "perturbation spikes" occurring in coincidence with the periods when the orbit crosses the Earth's shadow (see plots e.g. in Rubincam 1990; Scharroo et al. 1991). This correlation with the Earth eclipses is clearly an important clue to the physical cause of the perturbations — the most plausible candidates being of course the radiative effects. Therefore, a variety of *internal* and *external* radiative effects — using the terminology introduced in Sect. 1 — have been investigated in the last decade by several groups (Anselmo et al. 1983b; Barlier et al. 1986; Rubincam 1987; Afonso et al. 1989; Scharroo et al. 1991; Vokrouhlický et al. 1993b). It is now clear that several mechanisms contribute together to the observed long–periodic semimajor axis residuals. However, the quantitative models developed so far have achieved only a rather poor fit to the observations, and that at the cost of adopting unplausible or untestable assumptions, such as the large temperature gradient and the reflectivity asymmetry across the satellite invoked by Scharroo et al. (1991). This is the reason why we have decided to assess the possible contribution of the penumbra effect to the residuals. In order to do so, some preliminary comments are necessary.

Throughout this section, we will deal with the difference between the simple step–like model of the way eclipses interrupt the action of solar radiation pressure, and our more realistic theory of the penumbra transitions described in Sect. 2. Since the former is widely used in LAGEOS orbit analysis, whereas the real world includes the penumbra phenomena in their full complexity, we are going to call "penumbra effect" the *additional* (and unmodelled) perturbations arising from the more refined theory. However, we will not carry out a truly realistic study of this effect, which depends upon a number of parameters describing the (variable) state of the atmosphere, for which we have no direct observational knowledge. Our aim will just be that of answering the following semi–quantitative questions: is the contribution of the penumbra effect to LAGEOS' long–periodic semimajor axis residuals negligible? and if not, what are its typical order of magnitude and time dependence?

The typical magnitude of the direct radiation pressure acceleration on LAGEOS is 3×10^{-9} m/s^2 (we recall that the unmodelled residuals correspond to accelerations of the order of 10^{-12} m/s^2). The penumbra transitions extend over a typical duration of ≈ 100 sec, or about 10^{-2} of the orbital period. Hence the imbalance of the radiation accelerations over one orbit cannot exceed about 10^{-11} m/s^2. Actually, this upper limit is quite pessimistic: only the asymmetry between the entry (from sunlight to shadow) and the exit (from shadow to sunlight) transitions matters here, and the true average acceleration is likely to be more than one order of magnitude smaller than the upper limit given above. This will be confirmed by the numerical results described in the following. As we shall see, the corresponding accuracy requirements are not difficult to meet. However, one should be careful not to introduce systematic effects along the orbit that do not cancel out between the entry and the exit transitions, and could give raise to an artificial asymmetry.

First, let us analyse the pattern of the additional penumbra perturbations along a single revolution of the satellite. In Fig. 3 we have chosen 19 orbital revolutions close to the end of a shadow–crossing interval, which typically lasts $\approx$ 100 days for LAGEOS (whose orbital elements have been taken from Barlier et al. 1986). The curves labelled 1 correspond to the case when the orbit would still be predicted to penetrate the (assumedly cylindrical) Earth's shadow by the geometrical step–like model. These curves have two discontinuities with

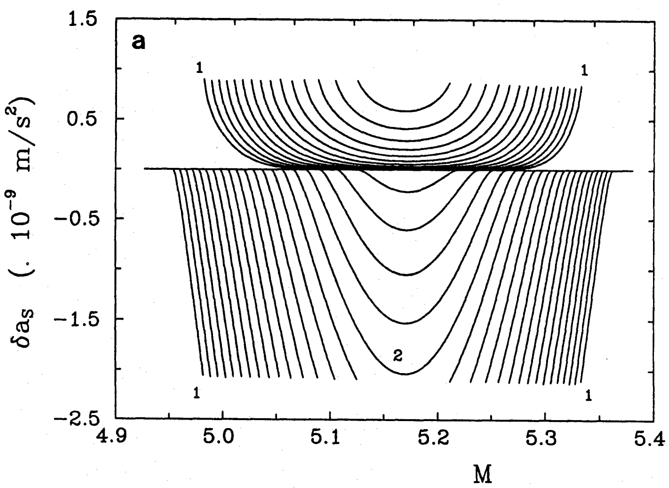

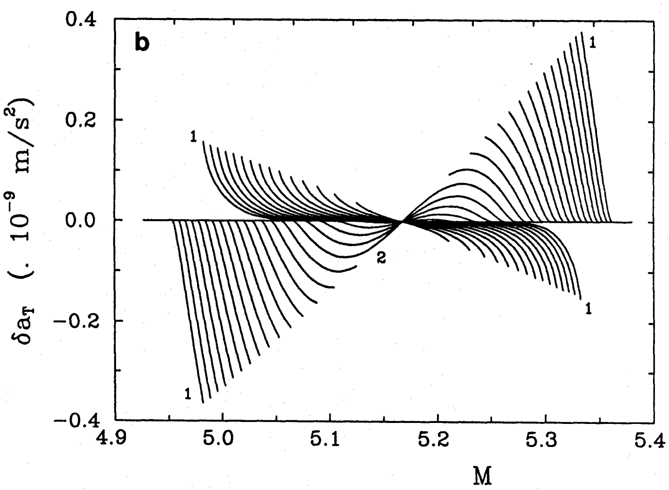

Fig. 3a and b. Difference between the values of the radial (δa_S, 3a) and transverse (δa_T, 3b) acceleration components due to solar radiation pressure acting during the penumbra transitions, computed with the approximate theory described in Sect. 2 and with the simple step–like model. The horizontal axis gives the mean anomaly along LAGEOS' orbit. The last 19 revolutions before the orbit ceases to cross the Earth's shadow are represented. At the beginning (curves labelled 1) the acceleration differences are discontinuous, as they change in sign at the points were the step–like transitions into and out of the shadow are assumed to occur. Later on (curves labelled 2) the curves become continuous, as a decrease of the solar flux is caused by penumbra even though the step–like geometrical model would predict that the satellite is always in full sunlight

the perturbation changing sign, at the points where the step–like transitions from light to darkness and *vice versa* would be assumed to occur. Since in this case both the radial and the transverse additional acceleration components change sign during a single transition, their averaged values can be expected to be much smaller than the magnitude of the radiation pressure perturbation — roughly 3×10^{-9} m/s^2, as mentioned earlier. This situation is typical for most of the duration of a shadow–crossing interval, with the penumbra signals associated with the shadow entry/exit separated by longer orbital arcs, which LAGEOS spends in the "geometrical shadow". The asymmetry between the additional perturbations undergone when the satellite is "geometrically" in sunlight and in shadow also vary, depending on the orientation of the orbit with respect to the shadow, but there is no qualitatively different feature.

An interesting situation occurs at the very edges (near the beginning or the end) of the shadow crossing periods, when the simple geometrical model would predict the orbit to be fully out of shadow, whilst according to the more realistic theory atmospheric processes cause some decrease of the solar flux — i.e., a penumbra effect — where the orbit grazes the shadow. Were the Sun to be observed from the standpoint of the satellite, it would be seen to enter nearly tangentially into the atmosphere (where atmospheric effects occur, such as deformation of the solar disk, refractive flux attenuation and absorption), without being totally eclipsed by the solid Earth. This peculiar geometrical configuration of the orbit lasts only several revolutions (typically 5, see Fig. 3) and therefore its long–term consequences are limited, but as we shall see it may give raise to significant perturbation spikes. This quasi–eclipse situation applies to the curves labelled 2 in Fig. 3. They are continuous, since no step–like transition occurs in the simple geometrical model. In this case, the additional radial component does not change sign and therefore its average value may become fairly large, whereas the averaged value of the transverse component remains smaller, because it still changes sign at the point where the solar centre gets closest to the Earth's surface.

Actually, it is easy to prove that any model based on a perfectly symmetrical shadow — e.g., that assuming a simple cylindrical shadow or a more complex one taking into account the atmosphere and the penumbra, but assuming the same atmospheric conditions over the whole Earth's surface — predicts that the one–revolution averaged transverse component of the additional penumbra perturbation is always zero for a circular orbit, and is demultiplied by the eccentricity for an elliptical orbit. This is due to the fact that for a circular orbit and a symmetrical shadow the additional transverse perturbation arising near the shadow entry is exactly cancelled out by that near the shadow exit. Since LAGEOS' orbital eccentricity is very small ($e \approx 0.004$), we need a global anisotropy of the atmospheric conditions (and hence of the optical properties of the atmosphere) to build up significant long–term effects on the semimajor axis. Such global (latitude–dependent) variations in the atmospheric conditions are plausible, for instance because meteorological seasons imply systematic differences in temperature, pressure, water vapor content and cloud coverage in the Northern vs. Southern hemispheres.

We note here a striking similarity between the penumbra and the albedo effect: as first pointed out by Anselmo et al. (1983a), the latter has also the property that its orbit–averaged transverse perturbation component would vanish for an isotropic Earth, hence the associated long–term semimajor axis variations depend just on subtle asymmetric features in the way the Earth scatters and reflects sunlight. Like in the case of the albedo effect, detailed meteorological data on these features are not available to us. Hence, we shall base our assessment of the

Table 1. Model for the season– and latitude–dependent variations of the atmospheric parameters

Earth surface conditions...	implying in summer ($\lambda_\odot = \pi/2$):
$T_0 = T_{00} + \Delta T_0 \sin\varphi_g \sin\lambda_\odot$	higher temperature
$p_0 = p_{00} + \Delta p_0 \sin\varphi_g \sin\lambda_\odot$	higher pressure
$T_0' = T_{00}' - \Delta T_0' \sin\varphi_g \sin\lambda_\odot$	larger (negative) temperature gradient
$p' = \Delta p'(1 - \sin\varphi_g \sin\lambda_\odot)$	lower humidity
$\chi = \chi^\star \times 10^{-\sin\varphi_g \sin\lambda_\odot}$	lower absorption coefficient

penumbra effect on a plausible phenomenological model of the variations (across the Earth and in time) of the atmospheric properties, without attempting any quantitative fit to the observed residuals.

Any plausible model for the atmospheric parameters (T_0, p_0, T_0', p') must include their variations with geographical latitude (φ_g)) and season (specified by the solar ecliptic longitude $\lambda_\odot$ measured the from vernal equinox, i.e. with $\lambda_\odot = 0$ corresponding to the spring equinox). Our choice for the dependence of the four parameters listed above on these two arguments is summarized in Tab. 1, where the mathematical formulae given in the left column are followed by qualitative explanations in the right column.

In general, one could expand the atmospheric parameters in a Fourier series of the two angular variables φ_g and $\lambda_\odot$. We have kept only those few terms which (i) do not involve completely unknown parameters, and (ii) are physically plausible (note that the assumedly polytropic character of the atmosphere involves some gauges in the variations of temperature and pressure, ruling out the existence of some Fourier terms). Obviously, we are oversimplifying the behaviour of the real atmosphere, but our model is refined enough for our current testing purposes. We adopt the following numerical values for the free parameters in Tab. 1: $T_{00} = 0°$C, $\Delta T_0 = 20°$C, $p_{00} = 760$ mm Hg, $\Delta p_0 = 30$ mm Hg, $T_{00}' = -0.005694$ K/m', $\Delta T_0' = 0.0008$ K/m', $\Delta p' = 30$ mm Hg.

Figs. 4a,b show the orbit–averaged radial and transverse acceleration components due to the penumbra effect. The latter component does not vanish only as a result of the asymmetry in the atmospheric parameters, as explained earlier, whereas the former one shows sharp extrema (spanning only a few days) near the edges of the shadow–crossing periods, due to the quasi–eclipse effect. The data refer to the real LAGEOS orbit starting at the satellite's launch in May 1976, and the first shadow–crossing interval occurred in the period from November 1976 to February 1977, as indicated by the dashed strip in Fig. 4b. This corresponds to one of the highest peaks in the observed residuals (see plots in Rubincam 1987; Scharroo et al. 1991). It is intriguing to note that this peak occurred in the winter season, when our model predicts maximum asymmetry between the Southern and Northern Earth hemispheres, and thus penumbra perturbations of maximum amplitude are generated. In general, the largest extrema of the curve giving the LAGEOS semimajor axis residuals

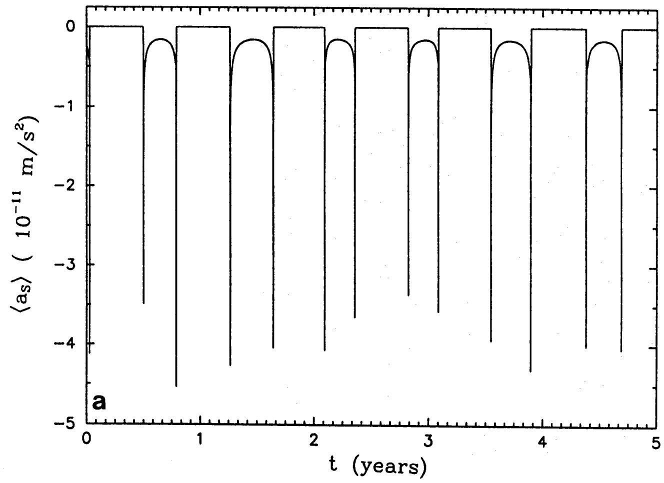

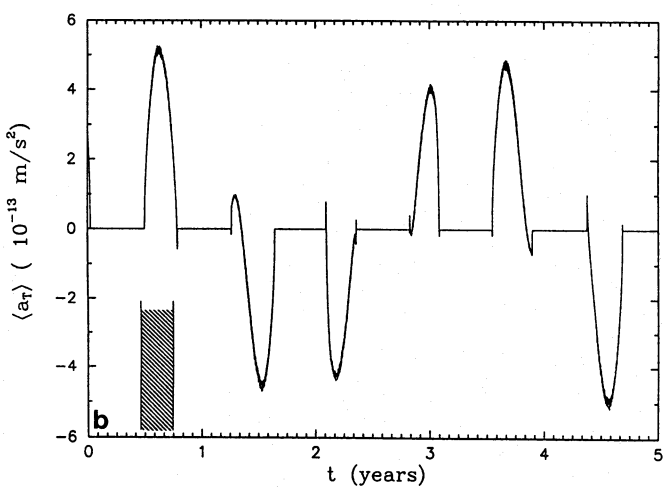

Fig. 4a and b. Orbit–averaged penumbra perturbations as a function of time for LAGEOS (starting at launch in May, 1976). The radial and transverse acceleration components are shown in parts **a** and —bf b, respectively

vs. time tend to occur roughly in the winter and summer seasons, when the asymmetry of the two Earth hemispheres is most pronounced. The succession of shadow–crossing intervals shows clearly the modulation of the penumbra effect perturbations by seasonal effects. When the shadow–crossing intervals occur out of the pure winter/summer periods, the $< a_T >$ amplitudes are smaller and changes of sign become possible.

It must be emphasized that the derivation of the approximate approach to the penumbra effect described in this paper is a compelling prerequisite to apply the theory to LAGEOS. Indeed, using the complete theory would have led to unacceptable CPU time requirements. The reason is the following: since the long–term semimajor axis effect is mainly due to tiny asymmetries of the penumbra phenomena at the shadow entries/exits, its computation involves subtracting from each other two large numbers, a task which is numerically hard to perform with high accuracy. Specifically, the magnitude of the instantaneous difference δa can reach about 2×10^{-9} m/s^2 (see Figs. 3), while the resulting averaged signal is of the order of 5×10^{-13} m/s^2 (see

Fig. 4). In order to achieve at least a 5% precision of the results, we had to take 0.1 sec integration timesteps in the penumbra phases, that is $\approx 10^{-5}$ of the orbital period!

Let us discuss now the precision of the results presented in Fig. 4b, namely those concerning the along–track component of the penumbra effect. Taking into account the instantaneous difference δa exceeding 10^{-9} m/s^2 and the 0.5% confidence level of the approximate theory (see Figs. 1 and 2), one might question the meaning of the resulting 5×10^{-13} m/s^2 residuals. However, it can be convincingly shown that these tiny residuals are indeed meaningful. Firstly, note that the average in Eq. (26) is performed over the penumbra interval only. As these intervals typically cover just some 2% of the whole orbital period, a typical value of 0.01% has to be expected for the one–revolution averaged acceleration difference between the complete and the approximate penumbra theories. Secondly, the δ–test expressed by Eq. (25) includes error contributions from all the three components, while here we are dealing with only one of them (the transverse component), whose magnitude is typically less than half of that of the radial component near the shadow entries/exits for LAGEOS' orbit. Moreover, the averaged value $< a >$ in Eq. (26) is roughly half of the maximum magnitude of the radiation pressure acceleration (3×10^{-9} m/s^2). As a result, one may estimate that the accuracy of the one–revolution averaged values of the along–track component computed by the approximate theory is of the order of 0.001%. Comparing this to the amplitude of the residuals (some 0.02% of the maximum magnitude of the perturbation), we can conclude that their relative error due to the use of the approximate theory does not exceed 5%. As discussed earlier, a similar error probably arises from the numerical averaging procedure. To check the validity of these estimates, we have computed averaged values of the penumbra along–track effect for several (randomly chosen) revolutions of LAGEOS employing the full (exact) theory given in Paper I, and compared the results with those obtained from the approximate theory. In no case we have found discrepancies greater than 5%, in agreement with the previous discussion.

Finally, it is interesting to consider the relation between the penumbra perturbations, as treated in Sect. 3, and the effect of solar eclipses studied by Rubincam & Weiss (1985). Generally speaking, the concept is the same — a simple treatment of the solar radiation pressure gives accurate results almost always along the satellite orbit, with the exception of short time intervals, when more complicated phenomena occur. Rubincam and Weiss showed that in spite of their short duration, solar occultations can give raise to detectable changes in the long–term behaviour of the orbit. Of course, penumbra effects induced by passages through the Earth's shadow occur much more frequently than solar eclipses (although they are shorter: some 200 sec compared to 20 minutes). However, the influence of the two effects is different for a more subtle reason: for the penumbra effect, the entry/exit compensation causes the net, one–revolution averaged perturbation to be much smaller than the size of the solar radiation forces, whereas this is obviously not the case for eclipses. On the other hand, the penumbra effect can accumulate for the whole duration of a shadow–crossing interval (typically 100 days for LAGEOS). As a result, the total semimajor axis effect over one of these intervals turns out to be comparable to that of the most prominent solar eclipses – $\Delta a \simeq 1.7$ cm (Rubincam & Weiss 1985).

4. Conclusions

The main results obtained in this paper can be summarized as follows.

(1) We have developed a working algorithm to model with great precision the changing solar radiation force exerted on a satellite during the passages from the full sunlight to the shadow cast by the Earth and *vice versa*. This algorithm removes the main obstacle (large CPU time requirements) to the application of the full–fledged theory presented in Paper I to satellite geodesy.

(2) The penumbra effect algorithm applied to LAGEOS shows conclusively that previously unmodelled long–term perturbations brought about by the solar radiation force have magnitudes reaching some 20% of the observed post–fit residuals. Although this effect cannot explain fully the extrema of the along–track unmodelled residuals of LAGEOS' orbit, it can in some instances amplify the effects due to other radiative mechanisms, such as the thermal thrust and albedo effects.

Some questions have not been fully answered or even addressed in this paper:

(1) In modelling the propagation of light rays in the Earth's atmosphere we have only included the simple *single–scattering* Rayleigh extinction, removing some energy from the solar light beam; any effect of *multiple–scattering* has been neglected.

(2) Similar penumbra phenomena occur in connection with the radiation pressure due to sunlight reflected from the Earth's surface (the albedo effect). This problem has to be dealt with numerically because of complex optical behaviour of the Earth's surface. We are going to investigate it in the next paper of this series.

Acknowledgements. We are grateful to R. Vilhena de Moraes for helpful comments. This work was partially supported by the Italian Space Agency (ASI). It was performed while one of the authors (P.F.) was staying at the Observatoire de la Côte d'Azur (OCA) thanks to the "G. Colombo" fellowship of the European Space Agency. D.V. gratefully acknowledges support from the European Community and hospitality by OCA, Dept. CERGA (Grasse, France).

References

Afonso G., Barlier F., Carpino M., et al., 1989, Ann Geophys. 7, 501
Anselmo L., Farinella P., Milani A., Nobili A.M. 1983a, A&A 117, 3
Anselmo L., Bertotti B., Farinella P., Milani A., Nobili A.M., 1983b, Celest. Mech. 29, 27
Barlier F., Carpino M., Farinella P., et al., 1986, Ann. Geophys. 4, 193
Chandrasekhar S., 1950, Radiative Transfer, Oxford Univ. Press, Oxford

Fliegel H.F., Gallini T.E., Swift E.R., 1992, J. Geoph. Res. 97, 559

Garfinkel B., 1944, AJ 50, 169

Garfinkel B., 1967, AJ 72, 235

Van de Hulst H.C., 1980, Multiple Light Scattering (Tables, Formulas, and Applications), Academic Press, New York

Klinkrad H., Koeck Ch., Renard P., 1990, ESA Journal (Vol. 14), 409

Link F., 1962, Bull. Astron. Inst. Czech. 13, 1

Link F., 1969, Eclipse Phenomena in Astronomy, Springer–Verlag, Berlin

McCartney E.J., 1976, Optics of the Atmosphere (Scattering by Molecules and Particles), J. Willey & Sons, New York

Mihalas D., 1970, Stellar Atmospheres, W.H. Freeman and Co., San Francisco

Milani A., Nobili A.M., Farinella, P. 1987, Non–Gravitational Perturbations and Satellite Geodesy, A. Hilger, Bristol

Peřestý R., Sehnal L., 1992, In–orbit microaccerelerometric experiment, presented at the 43rd congress of the International Astronautical Federation, Washington DC

Rubincam D.P., 1982, Celest. Mech. 26, 361

Rubincam D.P., 1987, J. Geoph. Res. 92, 1287

Rubincam D.P., 1988, J. Geoph. Res. 93, 13,805

Rubincam D.P., 1990, J. Geoph. Res. 95, 4881

Rubincam D.P., Weiss N.R., 1985, J. Geoph. Res. 90, 9399

Rubincam D.P., Weiss N.R., 1986, Celest. Mech. 38, 233

Scharroo R., Wakker K.F., Ambrosius B.A.C., Noomen R., 1991, J. Geophys. Res. 96, 729

Smith D.E., Dunn P.J., 1980, Geophys. Res. Lett. 7, 437

Vokrouhlický D., Farinella P., Lucchesi D., 1993a, Celest. Mech., 57, 225

Vokrouhlický D., Farinella P., Lucchesi D., 1993b, A&A, 280, 282

Vokrouhlický D., Farinella P., Mignard F., 1993c, A&A, 280, 295

This article was processed by the author using Springer-Verlag TEX A&A macro package 1992.